

Article

Synthesis and Structural Characterization of a New 1,2,3-Triazole Derivative of Pentacyclic Triterpene

Ewa Bębenek ^{1,*} , Monika Kadela-Tomanek ¹ , Elwira Chrobak ^{1,*} , Maria Jastrzębska ² and Maria Książek ³ 

¹ Department of Organic Chemistry, Faculty of Pharmaceutical Sciences in Sosnowiec, Medical University of Silesia, Katowice, 4 Jagiellońska Str., 41-200 Sosnowiec, Poland; mkadela@sum.edu.pl

² Silesian Center for Education and Interdisciplinary Research, Institute of Physics, University of Silesia, 75 Pułku Piechoty Str.1a, 41-500 Chorzów, Poland; maria.jastrzebska@us.edu.pl

³ Faculty of Science and Technology, Institute of Physics, University of Silesia in Katowice, 75 Pułku Piechoty Str.1a, 41-500 Chorzów, Poland; maria.ksiazek@us.edu.pl

* Correspondence: ebebenek@sum.edu.pl (E.B.); echrobak@sum.edu.pl (E.C.); Tel.: +48-32-364-16-66 (E.B.)

Abstract: The new 30-substituted triazole derivative of 3,28-*O,O'*-diacetylbetulin was obtained in the copper(I) catalyzed azide-alkyne cycloaddition (CuAAC). The title compound was characterized by NMR, IR, HR-MS, and X-ray diffraction techniques. The X-ray diffraction study showed that the 1,2,3-triazole derivative crystallizes in the orthorhombic space group $P2_12_12_1$, $Z = 4$, and unit cell parameters are as follows $a = 9.4860(10)$ Å, $b = 13.9440(2)$ Å, and $c = 30.2347(4)$ Å. The molecular packing is stabilized by intermolecular hydrogen interactions C-H ... O. The Hirshfeld surface analysis showed the presence of the O ... H interactions with a percentage of the 16.5% in the total Hirshfeld area. The MEP analysis showed that the nucleophilic regions are located near the oxygen atoms of the acyl and carbonyl groups of betulin moiety and the sulfur atom in the triazole linker. The HOMO and LUMO orbitals are located near the triazole moiety. The obtained results indicated that this new betulin derivative is more reactive with electrophilic than nucleophilic molecules.

Keywords: pentacyclic triterpenes; X-ray structure; Hirshfeld analysis



Citation: Bębenek, E.; Kadela-Tomanek, M.; Chrobak, E.; Jastrzębska, M.; Książek, M. Synthesis and Structural Characterization of a New 1,2,3-Triazole Derivative of Pentacyclic Triterpene. *Crystals* **2022**, *12*, 422. <https://doi.org/10.3390/cryst12030422>

Academic Editor: Waldemar Maniukiewicz

Received: 25 February 2022

Accepted: 14 March 2022

Published: 18 March 2022

Publisher's Note: MDPI stays neutral with regard to jurisdictional claims in published maps and institutional affiliations.



Copyright: © 2022 by the authors. Licensee MDPI, Basel, Switzerland. This article is an open access article distributed under the terms and conditions of the Creative Commons Attribution (CC BY) license (<https://creativecommons.org/licenses/by/4.0/>).

1. Introduction

Pentacyclic triterpenes are bioactive secondary metabolites found widely distributed throughout the plant kingdom. Betulin belongs to the lupane-type triterpenoids and is obtained in significant amounts from bark of white birch species (*Betula* spp.). This naturally derived product contains the 30-carbon skeleton consisting of four six-membered rings and one five-membered ring (Figure 1). Transformation of functional groups of betulin, such as isopropenyl moiety or C-3/C-28 hydroxyl group, gives the opportunity to design new derivatives [1,2]. Naturally occurring betulin and its semi-synthetic derivatives possess a broad range of pharmacological properties such as anticancer, antiviral, antimalarial, antimicrobial, antidiabetic, hepatoprotective, and anti-inflammatory activities. The different biological activities of pentacyclic triterpenoids may be due to the presence of following functional groups: ketone, ester, amino, oxime, sulfonate, and alkyne attached to the lupane skeleton. Unfortunately, the use of betulin as a potential therapeutic substance is limited by its poor solubility in water and low bioavailability [1,3–12].

It was observed that linking the parent structure of pentacyclic triterpenes with the 1,2,3-triazole ring makes it possible to improve their pharmacokinetic properties. Compounds containing a triazole ring exhibit a broad spectrum of biological activity. This is due to the possibility of binding to various enzymes and receptors by creating non-covalent interactions [13].

The triazole ring, one of the most important heterocyclic scaffolds, can be used as the bioisostere group of an amide, ester, or carboxyl group. Copper catalyzed azide-alkyne cycloaddition (CuAAC) leading to 1,2,3-triazole occurs under mild conditions

with high yield and allows simple product isolation. It should be mentioned that some compounds containing the 1,2,3-triazole system have been used in medicine as antibacterial (tazobactam) and anticancer (cefatrizine) drugs [12,14–17].

In 2009 the cycloaddition reaction was used for the first time in the synthesis of triazole derivatives of triterpenes. The triazole ring as an element connecting the basic triterpene skeleton with various types of substituents has been introduced at the positions C-3, C-28, and C-30. The solubility-increasing effect was observed for the triazole derivatives converted to conjugates with α - and β -cyclodextrin [17].

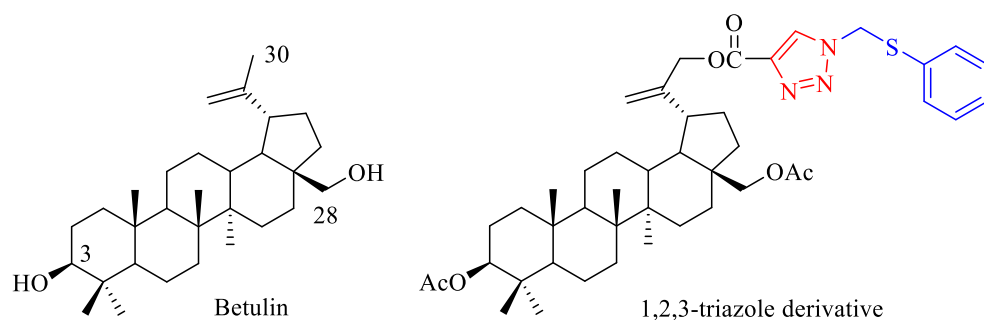


Figure 1. Chemical structure of betulin and 1,2,3-triazole derivative of 3,28-*O,O'*-diacetylbetulin.

In the present work, we described synthesis of new 30-substituted triazole derivative of 3,28-*O,O'*-diacetylbetulin. The chemical structure of 3,28-*O,O'*-diacetyl-30-(1-phenylthiomethyl-1*H*-1,2,3-triazol-4-yl)carbonylbetulin (Figure 1) was confirmed by NMR, IR, HR-MS, and X-ray analyze. Moreover, Hirshfeld and DFT calculations were used to obtain the electronic parameters of the new 1,2,3-triazole derivative.

2. Materials and Methods

2.1. General Methods

All commercial reagents were purchased from the Sigma-Aldrich (Sigma-Aldrich, Saint Louis, MO, USA). Melting point was measured with the Electrothermal IA 9300 melting point apparatus (Bibby Scientific Limited, Stone, Southhampton, GB). The NMR spectra were measured in deuterated chloroform as solvent using the Bruker Avance III 600 spectrometer (Bruker, Billerica, MA, USA). The chemical shifts are given in ppm (δ) and the coupling constants (J) in Hz. Multiplicities are indicated by the following abbreviations: singlet (s), doublet (d), and multiplet (m). The high-resolution mass spectral analysis was performed on a Bruker Impact II instrument (Bruker) using an atmospheric pressure chemical ionization APCI method (negative mode). The IR spectrum (KBr, pellet) was recorded using the IRAffinity-1 Shimadzu spectrometer (Shimadzu Corporation, Kyoto, Japan). The progress of reactions was monitored by TLC method (silica gel 60 254F plates, Merck). The spots were visualized by spraying with solution of 5% sulfuric (VI) acid and then heating to 100 °C. Triazole derivative was purified by a flash chromatography (Grace Reveleris Prep, Buchi, Flawil, Switzerland) using an ethyl acetate (A) and hexane (B) as mobile phase (40% A).

2.2. Synthesis of 3,28-*O,O'*-diacetyl-30-(1-phenylthiomethyl-1*H*-1,2,3-triazol-4-yl)carbonylbetulin 4

Synthesis of the intermediate compounds 1–3 (3,28-*O,O'*-diacetylbetulin 1, 3,28-*O,O'*-diacetyl-30-hydroxybetulin 2, 3,28-*O,O'*-diacetyl-30-propynoylbetulin 3) was performed according to the methods described previously [18–20].

Synthesis of 4: Azidomethyl phenyl sulfide (0.20 mmol) was added to the mixture of alkyne derivative 3 (0.11 g, 0.19 mmol) and copper(I) iodide (0.003 g, 0.001 mmol) in toluene (3.6 mL). The mixture was stirred under reflux for 72 h. The solvent was removed under reduced pressure and the residue was purified by flash chromatography using an ethyl acetate (A) and hexane (B) as mobile phase (40% A).

3,28-*O,O'*-diacetyl-30-(1-phenylthiomethyl-1*H*-1,2,3-triazol-4-yl)carbonylbetulin **4**.

Yield: 67%; m.p. 216–218 °C; R_f 0.46 (heksane/ethyl acetate, 3:2, *v/v*); ^1H NMR (600 MHz, CDCl_3) δ ppm: 0.85 (3H, s, CH_3), 0.86 (s, 3H, CH_3), 0.87 (s, 3H, CH_3), 0.96 (s, 3H, CH_3), 1.05 (s, 3H, CH_3), 2.07 (s, 3H, $\text{CH}_3\text{C}=\text{O}$), 2.09 (s, 3H, $\text{CH}_3\text{C}=\text{O}$), 2.43 (m, 1H, H-19), 3.83 (d, 1H, $J = 10.8$ Hz, H-28), 4.26 (d, 1H, $J = 10.8$ Hz, H-28), 4.47 (m, 1H, H-3), 4.84 (m, 2H, CH_2 , C-30), 5.03 (s, 1H, H-29), 5.05 (s, 1H, H-29), 5.69 (2H, s, CH_2), 7.33–7.53 (5H, m, H_{Ar}), 8.11 (1H, s, CH-triazole) (Figure S1-Supplementary materials); ^{13}C NMR (150 MHz, CDCl_3) δ ppm: 13.73, 15.02, 15.14, 15.48, 17.12, 19.87, 20.02, 22.65, 25.60, 25.98, 26.91, 28.71, 30.16, 33.09, 33.34, 36.02, 36.47, 36.77, 37.34, 39.88, 41.65, 42.81, 45.30, 48.54, 49.18, 53.32, 54.30, 54.95, 61.42, 79.86, 109.85, 126.78, 128.10, 128.25, 130.12, 130.16, 139.30, 147.14, 159.09, 169.99, 170.56. (Figure S2-Supplementary materials); IR (ν_{max} cm^{-1} KBr): 2954, 1735, 1448, 1242 (Figure S3-Supplementary materials); HR-MS (APCI) m/z : $\text{C}_{44}\text{H}_{61}\text{N}_3\text{O}_6\text{S} [\text{M}-\text{H}]^-$, Calcd. 758.4203; Found 758.4196 (Figure S4-Supplementary materials).

2.3. Determination of Crystal Structure

2.3.1. X-ray Diffraction Experiment

Colorless single crystals of good quality were preselected under a polarized light microscope. The single-crystal X-ray experiment was performed at 100 K. The data for compound **4** were collected using a SuperNova diffractometer (Agilent Technologies currently Rigaku Oxford Diffraction) with Atlas CCD detector. The controlling of the measurement and data reduction was performed by CrysAlis^{Pro} software [20]. The same program was used to determine and refine the lattice parameters [21].

2.3.2. Refinement

The crystal structure was determined using the direct methods with SHELXS-2013 program and then the solution was refined using SHELXL-2014/6 program [22]. H atoms were treated as riding atoms in geometrically idealized positions, fixing the C-H bond lengths at 1.00, 0.99, 0.95, and 0.98 Å for methine CH, methylene CH_2 , terminal methylene CH_2 , and methyl CH_3 atoms, respectively, and with $U_{\text{iso}}(\text{H}) \frac{1}{4} = 1.5U_{\text{eq}}(\text{C})$ for methyl H atoms or $1.2U_{\text{eq}}(\text{C})$ otherwise.

Crystal structure of compound **4** was deposited at the Cambridge Crystallographic Data Center, with deposit number CCDC 2153148 and is available free of charge via www.ccdc.cam.ac.uk/data_request/cif (accessed date: 10 March 2022).

2.4. Hirshfeld Surface Analysis

The percentages of the intermolecular contacts in crystal structure of **4** were designated using the Hirshfeld surface analyses. The colors of 3D d_{norm} indicate different regions on this surface, i.e., red regions represent the closer contacts and negative d_{norm} value, blue regions correspond to longer contacts and positive d_{norm} values. The 3D and 2D plots were performed by Crystal-Explorer v.3.1 program [23]. Both *de* and *di* parameters are responsible for the normalized contact distance (d_{norm}).

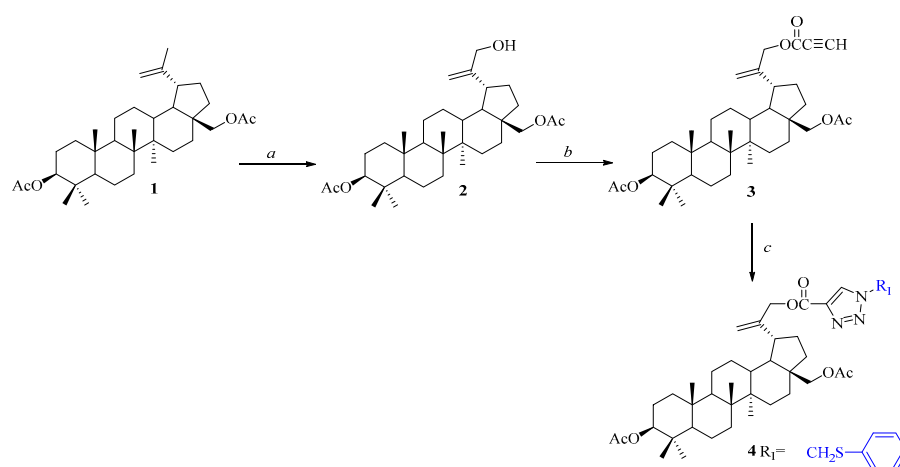
2.5. Computational Details

Calculations of the electronic structure of **4** were performed *in silico* using the DFT method implemented in the Gaussian 09 program package [24]. The initial molecular geometry of **4** was taken from the X-ray crystallographic data. Geometry optimization was performed using the B3LYP exchange-correlation functional with the 6-311G+(d,p) basis set. All obtained results were visualized in the GaussView, Version 5 software package [25]. The superposition of both structures, i.e. experimental obtained by single crystal X-ray diffraction and optimized is shown in Figure S5 (Supplementary materials).

3. Results and Discussion

3.1. Synthesis of Compound 4

Triterpenes 1–3 were prepared according to the procedures previously described in the literature [17–19]. The allylic oxidation of the isopropenyl group in 3,28-*O,O'*-diacetylbetulin 1 using *m*-chloroperbenzoic acid (*m*-CPBA) in refluxing chloroform provided the 3,28-*O,O'*-diacetyl-30-hydroxybetulin 2. The esterification of the C-30 hydroxy group of compound 2 was accomplished using propynoic acid, DCC (*N,N'*-dicyclohexylcarbodiimide) and DMAP (4-dimethylaminopyridine) in dichloromethane to provide 30-propynoylated derivative 3. The resulting alkyne derivative 3 was further functionalized to triazole 4 via click reaction in refluxed toluene in the presence of azidomethyl phenyl sulfide and copper(I) iodide [26,27]. Synthesis of 30-substituted triazolyl derivative 4 is depicted in Scheme 1.



Scheme 1. Reagents and conditions: (a) *m*-CPBA (*m*-chloroperbenzoic acid), CHCl_3 (chloroform), reflux, 8 h; (b) $\text{HC}\equiv\text{CCOOH}$ (propynoic acid), CH_2Cl_2 (dichloromethane), DCC (*N,N'*-dicyclohexylcarbodiimide), DMAP (4-dimethylaminopyridine), from $-10\text{ }^\circ\text{C}$ to room temperature, 24 h (c) PhSCH_2N_3 , (azidomethyl phenyl sulfide), CuI [copper(I) iodide], toluene, reflux, 72 h.

3.2. Crystal Structure of Compound 4

The single crystal of 4 was grown by slow evaporation at room temperature from acetonitrile solution. Molecular structure with atom numbering for the crystal is presented in Figure 2. The crystallographic data for 4 are summarized in Table 1.

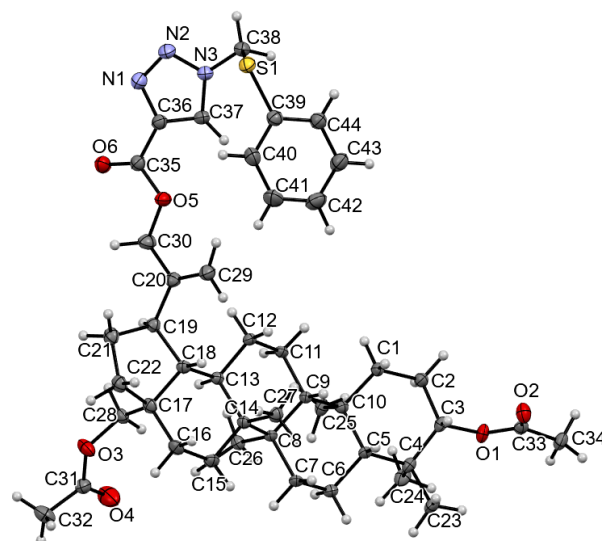


Figure 2. Molecular structure with atom numbering of compound 4.

The unit cell of **4** contains four molecules ($Z = 4$) and is presented in Figure 3.

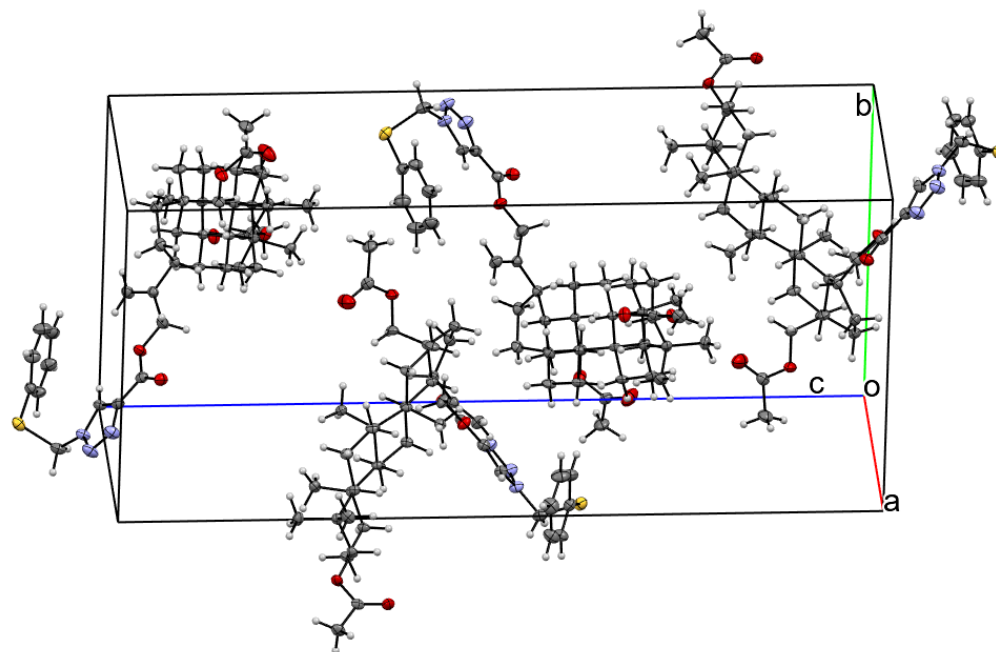


Figure 3. Molecular packing of unit cell for **4**.

The six-membered rings of betulin scaffold adopt chair conformation. The cyclopentane ring assumes conformation of the twisted envelope. The torsion angle C19-C20-C29-C30 describing the orientation of the isopropenyl group arrangement in relation to the five-membered ring of **4** is equal to -176.50° . The introduction of large substituent at the C-30 position in **4** caused a significant change in the arrangement of this group compared with the 3,28-*O,O'*-diacetylbetulin (C19-C20-C29-C30 = 177.69° , [28]). The selected geometric parameters (e.g., bond length, bond angles, and torsion angles) are presented in Tables S1 and S2 (Supplementary materials).

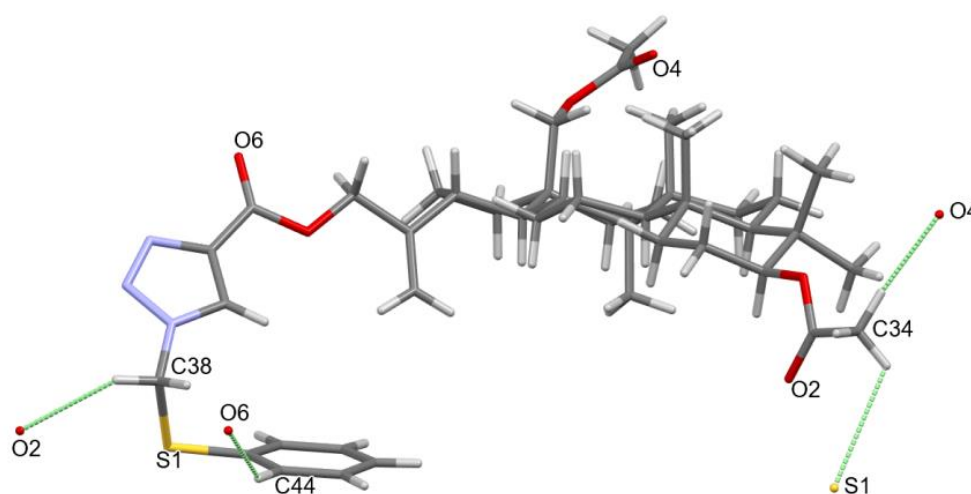
Table 1. Crystal data and structure refinement for **4**.

Compound	4
CCDC deposition number	2,153,148
Chemical formula	$C_{44}H_{61}N_3O_6S$
<i>Mr</i>	760.01
Solvent	CH_3CN
Crystal system, space group	orthorhombic; $P2_12_12_1$
Temperature (K)	100
<i>a, b, c</i> (Å)	9.4860(10); 13.9440(2); 30.2347(4)
α, β, γ [°]	90; 90; 90
$V(\text{Å}^3)$	3999.23(9)
<i>Z</i>	4
<i>Z'</i>	1
D _{calc} (g/cm ³)	1.262
Radiation type	Cu <i>K</i> α
μ (mm ⁻¹)	1.13
Crystal size (mm ³)	0.02 × 0.04 × 0.32
<i>R</i> _{int}	0.0304
<i>R</i> _{sigma}	0.0226
No. reflns. ($5.8^\circ \leq 2\theta \leq 145.0^\circ$)	19,516
Unigue reflns.	7268
λ (Å)	1.5418

Table 1. *Cont.*

Compound	4
GOOF (F ²)	1.053
θ range for data collection (°)	2.9 to 72.5
R1	0.0383
wR2	0.1038

Molecules of **4** are linked to each other by weak C-H ... O hydrogen bonds. The hydrogen bond parameters are shown in Table 2. All intermolecular hydrogen interactions C-H ... O determining molecular packing are presented in Figure 4.

**Figure 4.** The main weak C-H ... O hydrogen bonds found in the crystal of **4**.

The molecular structure of compound **4** is stabilized by weak intermolecular hydrogen bonds (Table 2; Figure 4). The basic betulin structures are linked to each other in a “head to tail” system through C-H–O bonds formed between atoms C34 and O4 from the next molecule. Molecules connected in this way form a spring-like structure along the a-axis (Figure 5A). Additional stabilization of the crystal structure is provided by the C38–H38–O2, C44–H44–O6, C34–H34C–S1, and C43–H43–N2 bonds (Figure 5B) as well as π – π interactions between the triazole ring and the phenyl substituent (Figure S6, Supplementary Materials).

Table 2. Selected weak C-H ... O hydrogen bonds in **4**.

Nr	D-H ... A	D-H [Å]	H ... A [Å]	D ... A [Å]	<(DHA)	Symmetry Codes
1	C34-H34B ... O4	0.98	2.39	3.305(4)	155.5	$-x + 1, y + 1/2, -z + 1/2$
2	C34-H34C ... S1	0.98	2.98	3.517(3)	116.0	$x - 3/2, -y + 5/2, -z$
3	C38-H38A ... O2	0.99	2.59	3.299(4)	128.6	$x + 3/2, -y + 5/2, -z$
4	C44-H44 ... O6	0.95	2.65	3.460(4)	143.2	$x - 1/2, -y + 5/2, -z$
5	C43-H43 ... N2	0.95	2.63	3.450(4)	144.7	$-1 + x, y, z$

D: donor, A: acceptor. Distances DH, HA, DA, are in Å and DHA angles are in degrees.

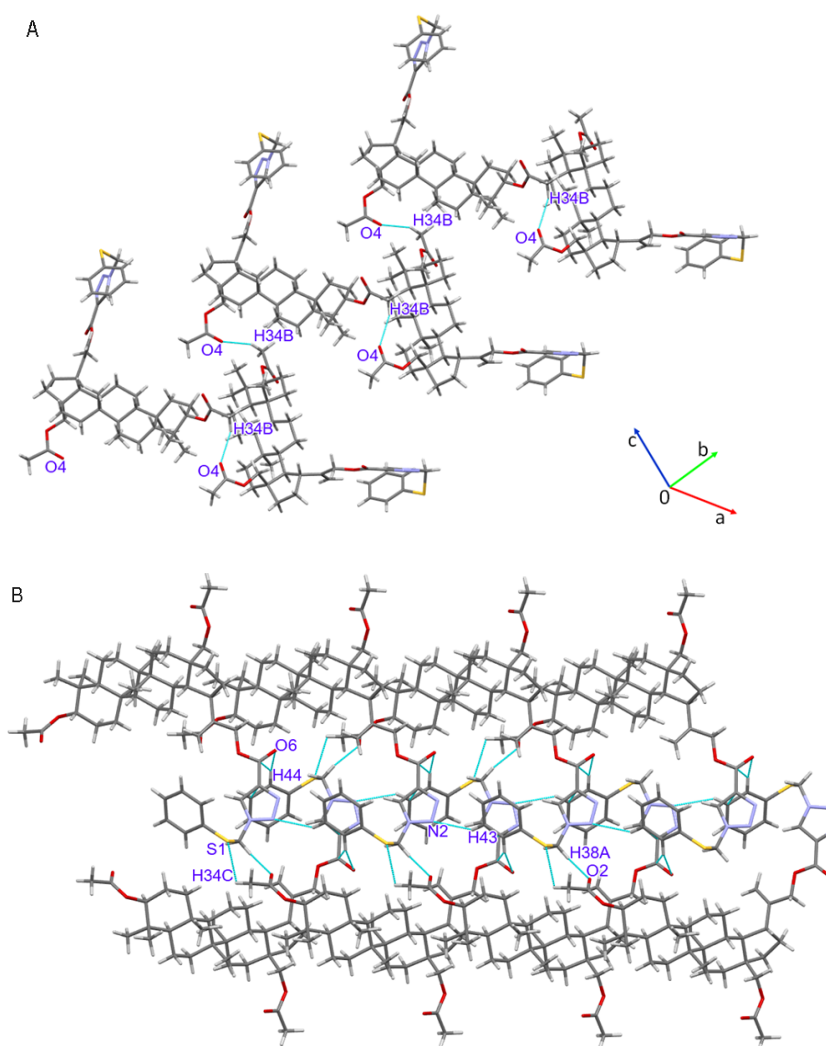


Figure 5. The intermolecular (A) hydrogen C34-H34B ... O4 bonds and (B) the other hydrogen bonds and π - π interactions.

3.3. Hirshfeld Surface

Analysis of the short and long interactions in crystal structure is possible through the Hirshfeld surface analysis. The 3D surface is characterized by different colors, which indicate different norm values. The negative value of d_{norm} relating to close contacts is represented by red color, while its positive value meaning longer interaction is represented by blue color. The white region means that the d_{norm} is zero (Figure 6) [29].

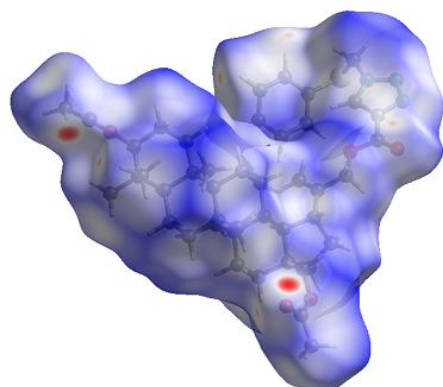


Figure 6. The Hirshfeld surface for 4. The d_{norm} is viewed from the c-axis.

Comparing Figures 4 and 6 shows that the red regions are localized near the acyl groups at positions C-3 and C-28 containing carbonyl oxygen atoms, which create the hydrogen bond. The triazole ring involving in long distance interaction, is visualized by blue color. Figure 7a–d presents the quantitative analysis of intermolecular contacts using 2D fingerprint plots for compound 4. The 2D fingerprint plots show that the intermolecular interactions are dominated by the O–H interaction. The sharp spike in Figure 7c indicates the presence of the O...H hydrogen bonds. The N...H and C...H interactions comprise 7.5% and 8.0% of the total Hirshfeld surface, respectively. The full 2D fingerprint plot for 4 is presented in Supplementary Materials (Figure S7). All interactions observed for 4 are summarized in Table 3 with their percentage contributions to the surface.

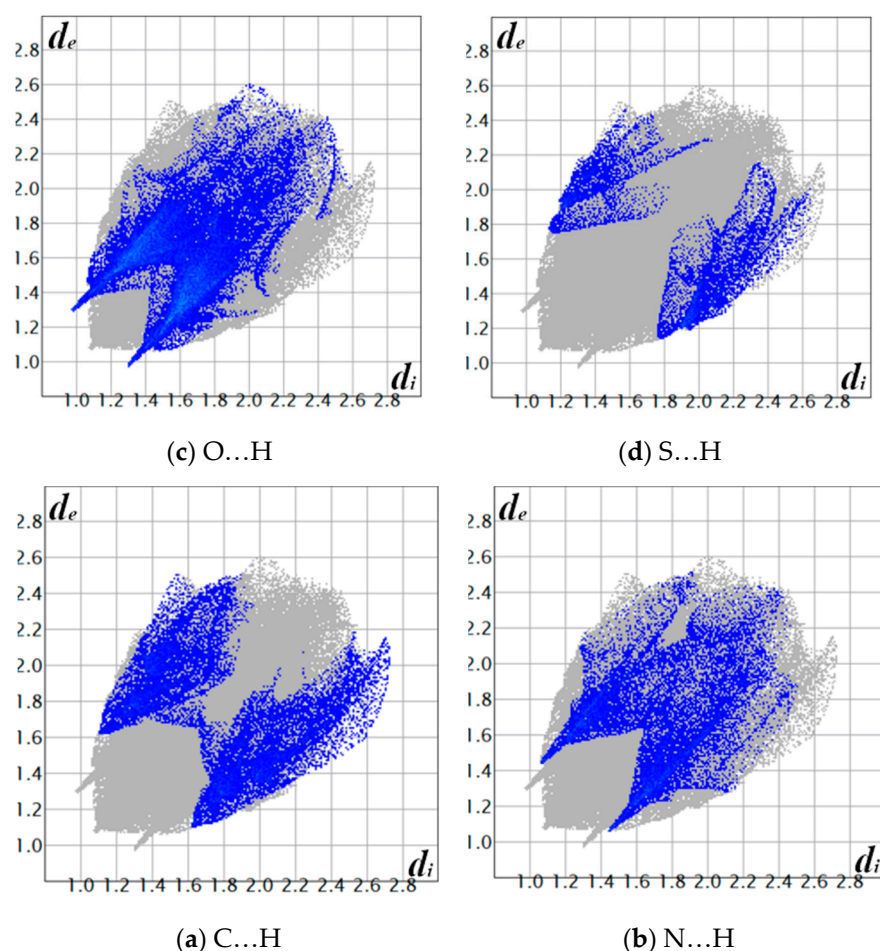


Figure 7. Fingerprint plots of (a) C...H, (b) N...H, (c) O...H, (d) S...H for 4.

Table 3. Percentage contributions of interatomic contacts to the Hirshfeld surface for 4.

Contacts	Contribution (%)
C...H	8.0
N...H	7.5
O...H	16.5
S...H	3.9
S...O	0.3
N...C	0.8
C...C	0.2

3.4. Molecular Electrostatic Potential Analysis

The charge arrangement in molecules is usually analyzed by determining the molecular electrostatic potential (MEP) map. The different colors on the MEP mean different values of the electrostatic potential. The red and blue colors represent the nucleophilic and electrophilic regions, respectively, while the light green color represents the charge-neutral region [30]. The negative potential regions are located in four main areas. The first and second areas contain an acyl group at the C-3 and C-28 positions, respectively. The third area includes the carbonyl group at the C-30 position and the triazole ring. The fourth area contains a sulfur atom. The positive potential region is located near the phenyl ring. The charge neutral region contains the betulin scaffold (Figure 8).

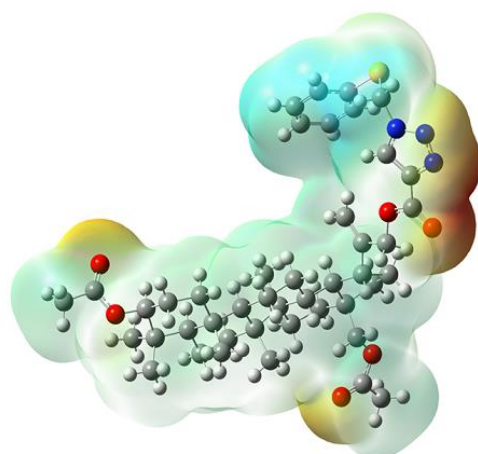


Figure 8. Molecular electrostatic potential (MEP) map for **4**.

In the first and second areas, two potential minima are observed (-1.09 , -2.07) eV and (-0.98 , -1.96) eV, respectively. In the third area four potential minima can be observed, two near the carbonyl group at the C-30 position (-0.54 eV and -1.96 eV) and the next two near the triazole ring (-2.79 eV and -2.07 eV). The potential minimum in the fourth area is -2.94 eV. The MEP surface of betulin described by Kazachenko shows two nucleophilic areas at the oxygen atoms in the C-3 and C-28 positions [31]. Comparing results for molecules **4** and betulin it can be seen, that introduction of the triazole ring at the C-30 position leads to formation of an additional nucleophilic area. The similar area of increasing electron density near the triazole ring was observed in the previously obtained triazole derivatives of betulin. These compounds were characterized by high anticancer activity. It has been observed, that the interaction of a compound with a biological target through the hydrogen and hydrophobic interactions depends on the system of nucleophilic and electrophilic regions in the molecule [32].

3.5. Molecular Properties of **4**

The density functional theory (DFT) implemented in Gaussian software was used to calculate some molecular properties of **4** [24]. The selected parameters are collected in Table 4. The molecular polarization and arrangement of the charges are described by a dipole moment. The total molecular dipole moment of **4** is equal to 5.9024 D. Comparing 3D components of the dipole moment shows that the highest negative value is for x -axis component μ_x . The molecular energy levels of **4** show that the 205 of 1163 molecular orbitals are occupied. The HOMO and LUMO orbitals show the ability of molecules to donate or acquire an electron, respectively. As shown in Figure 9, the HOMO and LUMO orbitals for **4** are delocalized on the triazole moiety. The high HOMO (-6.900 eV) and low LUMO energy levels (-1.412 eV) show that the molecule **4** is more reactive with electrophilic than nucleophilic molecules. The energy gap (ΔE) suggests that the molecule **4** has kinetic stability and is less polarizable [33].

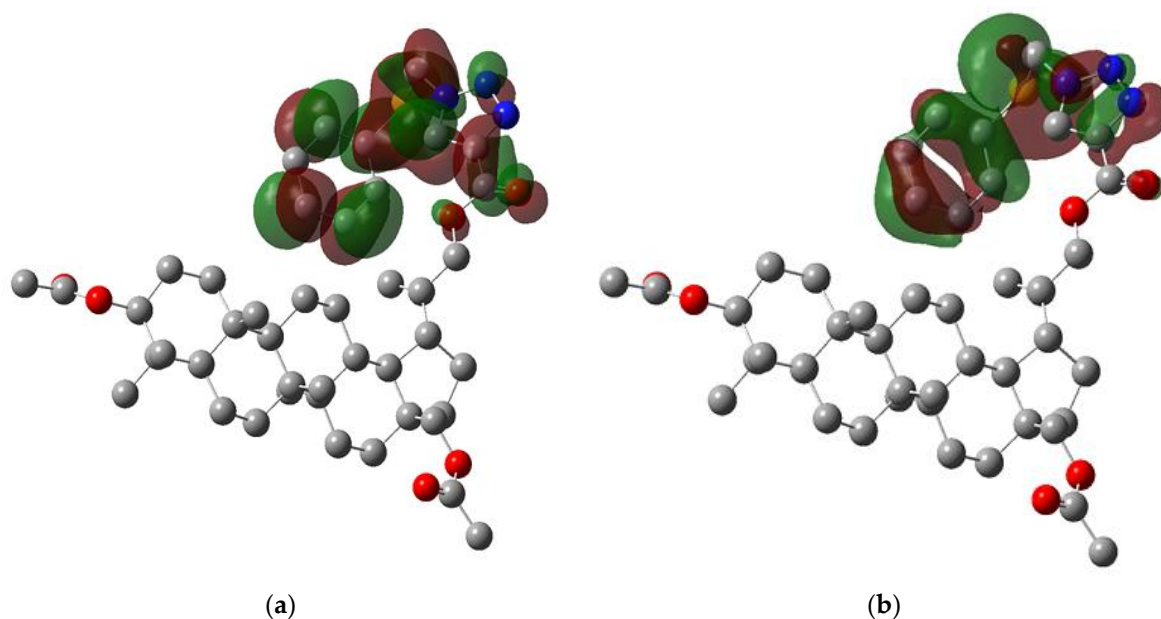


Figure 9. The molecular orbitals of 4: (a) LUMO; (b) HOMO.

Energies of the HOMO and LUMO orbitals were used to calculate the global reactivity descriptors such as ionization potential (I), electron affinity (A), hardness (η), softness (s), chemical potential (μ), electronegativity (χ), and electrophilicity index (ω) [34]. The obtained values are presented in Table 4.

Table 4. Calculated molecular properties of 4.

Parameters	6-311G+(d,p)
	Compound 4
SCF Energy (kcal/mol)	−74,208.4052
Field independent dipole moment (Debye)	
μ_x	−4.4518
μ_y	−1.8292
μ_z	3.4166
μ_{total}	5.9024
Fourier molecular orbital energies (eV)	
E_{HOMO}	−6.900
E_{LUMO}	−1.412
$\Delta E_{LUMO}-E_{HOMO}$	5.488
Global reactivity descriptors (eV)	
Ionization potential (I)	6.901
Electron affinity (A)	1.416
Hardness (η)	2.742
Chemical potential (μ)	−4.158
Electronegativity (χ)	4.158
Electrophilicity index (ω)	3.152

The chemical modification of betulin molecule into compound 4 increases the electrophilicity index from 1.223 eV [31] to 4.158 eV. The introduction of substituents at the C-3, C-28, and C-30 positions in the derivative 4 reduces the chemical potential (μ) from −2.947 [31] to −4.158 compared with betulin. The global reactivity descriptors show that 4 has high molecular stability. Moreover, the chemical potential and the electrophilicity index show also that 4 has a tendency to gain electrons [35].

4. Conclusions

The 3,28-*O,O'*-diacetyl-30-(1-phenylthiomethyl-1*H*-1,2,3-triazol-4-yl)carbonylbetulin **4** was synthesized by the alkyne-azide cycloaddition (CuAAC). Spectroscopy data and X-ray diffraction studies confirmed the chemical structure of compound **4**. It has been shown that the intermolecular hydrogen interactions C-H . . . O determine molecular packing in the crystal structure. The Hirshfeld surface analysis allowed the percentage of intermolecular contacts to be determined. The MEP map showed the electrophilic and nucleophilic areas for 1,2,3-triazole derivative **4**. The negative potential regions were located near the oxygen atoms of the betulin moiety and the sulfur atom in the triazole linker. Analysis of the HOMO and LUMO orbitals showed that the derivative **4** is more reactive with electrophilic than nucleophilic molecules.

Supplementary Materials: The following supporting information can be downloaded at: <https://www.mdpi.com/article/10.3390/cryst12030422/s1>, Figures S1–S4. ¹H NMR, ¹³CNMR, IR, and HR-MS for compounds **4**. Table S1: Selected bond lengths (Å) for compounds **4**. Table S2: Selected angle (degree) for compounds **4**. Figure S5: Atom by atom superimposition of X-ray structure (yellow) and calculate structure (grey). Figure S6: Intermolecular orientation of triazole and phenyl centroids showing π - π interactions. Figure S7: The full 2D fingerprint plot for **4**. check CIF report.

Author Contributions: E.B. and E.C. conceptualization, writing—original draft preparation, investigation, formal analysis, writing—review and editing; M.K.-T. software, formal analysis, writing—original draft preparation, visualization; M.J. methodology, writing—review and editing; M.K. validation, formal analysis. All authors have read and agreed to the published version of the manuscript.

Funding: This research received no external funding.

Institutional Review Board Statement: Not applicable.

Informed Consent Statement: Not applicable.

Data Availability Statement: Not applicable.

Acknowledgments: This research was supported by The Medical University of Silesia in Katowice Grant nos. PCN-1-009/N/1/F and PCN-1-010/N/1/F.

Conflicts of Interest: The authors declare no conflict of interest.

References

1. Amiri, S.; Dastghaib, S.; Ahmadi, M.; Mehrbod, P.; Khadem, F.; Behrouj, H.; Aghanoori, M.R.; Machaj, F.; Ghamsari, M.; Rosik, J.; et al. Betulin and its derivatives as novel compounds with different pharmacological effects. *Biotechnol. Adv.* **2020**, *38*, 107409–107447. [[CrossRef](#)] [[PubMed](#)]
2. Harun, N.H.; Septama, A.W.; Ahmad, W.A.N.W.; Suppian, R. Immunomodulatory effects and structure-activity relationship of botanical pentacyclic triterpenes: A review. *Chin. Herb. Med.* **2020**, *12*, 118–124. [[CrossRef](#)]
3. Grishko, V.V.; Tolmacheva, I.A.; Nebogatikov, V.O.; Galaiko, N.V.; Nazarov, A.V.; Dmitriev, M.V.; Ivshina, I.B. Preparation of novel ring-A fused azole derivatives of betulin and evaluation of their cytotoxicity. *Eur. J. Med. Chem.* **2017**, *125*, 629–639. [[CrossRef](#)] [[PubMed](#)]
4. Kazakova, O.; Smirnova, I.; Tret'yakova, E.; Csuk, R.; Hoenke, S.; Fischer, L. Cytotoxic potential of α -azepano- and 3-amino-3,4-*seco*-triterpenoids. *Int. J. Mol. Sci.* **2021**, *22*, 1714. [[CrossRef](#)] [[PubMed](#)]
5. Pęczak, P.; Orzechowska, B.; Chrobak, E.; Boryczka, S. Novel betulin dicarboxylic acid ester derivatives as potent antiviral agents: Design, synthesis, biological evaluation, structure-activity relationship and in-silico study. *Eur. J. Med. Chem.* **2021**, *225*, 113738–113750. [[CrossRef](#)] [[PubMed](#)]
6. Karagöz, A.Ç.; Leidenberger, M.; Hahn, F.; Hampel, F.; Friedrich, O.; Marschall, M.; Kappes, B.; Tsogoeva, S.B. Synthesis of new betulinic acid/betulin-derived dimers and hybrids with potent antimalarial and antiviral activities. *Bioorg. Med. Chem.* **2019**, *27*, 110–115. [[CrossRef](#)]
7. Myszk, H.; Grzywacz, D.; Zdrowowicz, M.; Spisz, P.; Butowska, K.; Rak, J.; Piosik, J.; Jaśkiewicz, M.; Kamysz, W.; Liberek, B. Design, synthesis and biological evaluation of betulin-3-yl 2-amino-2-deoxy- β -D-glycopyranosides. *Bioorg. Chem.* **2020**, *96*, 103568–103574. [[CrossRef](#)]
8. Kazakova, O.; Lopatina, T.; Giniyatullina, G.; Mioc, M.; Soica, C. Antimycobacterial activity of azepanobetulin and its derivative: In vitro, in vivo, ADMET and docking studies. *Bioorg. Chem.* **2020**, *104*, 104209–104217. [[CrossRef](#)]
9. Oboh, M.; Govender, L.; Siwela, M.; Mkhwanazi, B.N. Anti-diabetic potential of plant-based pentacyclic triterpene derivatives: Progress made to improve efficacy and bioavailability. *Molecules* **2021**, *26*, 7243. [[CrossRef](#)]

10. Buko, V.; Zavodnik, I.; Palecz, B.; Stepniak, A.; Kirko, S.; Shlyahatun, A.; Misiuk, W.; Belonovskaya, E.; Lukivskaya, O.; Naruta, E.; et al. Betulin/2-hydroxypropyl- β -cyclodextrin inclusion complex: Physicochemical characterization and hepatoprotective activity. *J. Mol. Liq.* **2020**, *309*, 113118–113127. [CrossRef]
11. Li, J.; Jiang, B.; Chen, C.; Fan, B.; Huang, H.; Chen, G. Biotransformation of betulin by *Mucor subtilissimus* to discover anti-inflammatory derivatives. *Phytochemistry* **2019**, *166*, 112076–112081. [CrossRef]
12. Kuczynska, K.; Bończak, B.; Rárová, L.; Kvasnicová, M.; Strnad, M.; Pakulski, Z.; Cmoch, P.; Fiałkowski, M. Synthesis and cytotoxic activity of 1,2,3-triazoles derived from 2,3-*seco*-dihydrobetulin via a click chemistry approach. *J. Mol. Struct.* **2022**, *1250*, 131751–131765. [CrossRef]
13. Csuk, R.; Niesen-Barthel, A.; Schäfer, R.; Barthel, A.; Al-Harrasi, A. Synthesis and antitumor activity of ring A modified 11-keto- β -boswellic acid derivatives. *Eur. J. Med. Chem.* **2015**, *92*, 700–711. [CrossRef] [PubMed]
14. Grymel, M.; Pastuch-Gawołek, G.; Lalik, A.; Zawojak, M.; Boczek, S.; Krawczyk, M.; Erfurt, K. Glycoconjugation of betulin derivatives using copper-catalyzed 1,3-dipolar azido-alkyne cycloaddition reaction and a preliminary assay of cytotoxicity of the obtained compounds. *Molecules* **2020**, *25*, 6019. [CrossRef]
15. Kumar, S.; Sharma, B.; Mehra, V.; Kumar, V. Recent accomplishments on the synthetic/biological facets of pharmacologically active 1H-1,2,3-triazoles. *Eur. J. Med. Chem.* **2021**, *212*, 113069–113100. [CrossRef] [PubMed]
16. Xu, Z.; Zhao, S.J.; Liu, Y. 1,2,3-Triazole-containing hybrids as potential anticancer agents: Current developments, action mechanisms and structure-activity relationships. *Eur. J. Med. Chem.* **2019**, *183*, 111700–111736. [CrossRef] [PubMed]
17. Csuk, R.; Deigner, H.P. The potential of click reactions for the synthesis of bioactive triterpenes. *Bioorg. Med. Chem. Lett.* **2019**, *29*, 949–958. [CrossRef] [PubMed]
18. Deng, Y.; Snyder, J.K. Preparation of a 24-nor-1,4-dien-3-one triterpene derivative from betulin: A new route to 24-nortriterpene analogues. *J. Org. Chem.* **2002**, *67*, 2864–2873. [CrossRef] [PubMed]
19. Huang, F.Y.; Chung, B.Y.; Bentley, M.D.; Alford, A.R. Colorado potato beetle antifeedants by simple modification of the birch bark triterpene betulin. *J. Agric. Food Chem.* **1995**, *43*, 2513–2516. [CrossRef]
20. Chrobak, E.; Bębenek, E.; Marciniak, K.; Kadela-Tomanek, M.; Siudak, S.; Latocha, M.; Boryczka, S. New 30-substituted derivatives of pentacyclic triterpenes: Preparation, biological activity, and molecular docking study. *J. Mol. Struct.* **2021**, *1226*, 129394–129404. [CrossRef]
21. CrysAlisPro. Version 1.171.38.41q. Rigaku Oxford Diffraction. 2015. Available online: <https://www.rigaku.com/en/products/smc/crysalis> (accessed on 21 November 2021).
22. Sheldrick, G.M. Crystal structure refinement with SHELXL. *Acta Cryst. C* **2015**, *71*, 3–8. [CrossRef] [PubMed]
23. Wolff, S.; Grimwood, D.J.; McKinnon, J.; Jayatilaka, D.; Spackman, M. *CrystalExplorer 3.0*; University of Western Australia: Perth, Australia, 2012.
24. Frisch, M.J.; Trucks, G.W.; Schlegel, H.B.; Scuseria, G.E.; Robb, M.A.; Cheeseman, J.R.; Scalmani, G.; Barone, V.; Mennucci, B.; Petersson, G.A.; et al. *Gaussian 09, Revision A.02*; Gaussian Inc.: Wallingford, CT, USA, 2009.
25. Dennington, R.; Keith, T.; Millam, J. *GaussView, Version 5*; Semichem Inc.: Shawnee Mission, KS, USA, 2009.
26. Bębenek, E.; Jastrzębska, M.; Kadela-Tomanek, M.; Chrobak, E.; Orzechowska, B.; Zwolińska, K.; Latocha, M.; Mertas, A.; Czuba, Z.; Boryczka, S. Novel triazole hybrids of betulin: Synthesis and biological activity profile. *Molecules* **2017**, *22*, 1876. [CrossRef]
27. Bębenek, E.; Kadela-Tomanek, M.; Chrobak, E.; Latocha, M.; Boryczka, S. Novel triazoles of 3-acetylbetulin and betulone as anticancer agents. *Med. Chem. Res.* **2018**, *27*, 2051–2061. [CrossRef] [PubMed]
28. Mohammedi, I.E.; Choudhary, M.I.; Ali, S.; Anjum, S. Atta-ur-Rahman. 20(29)-Lupene-3 β ,28 β -diacetate. *Acta Crystallogr.* **2006**, *E62*, o1352–o1354.
29. Spackman, M.; McKinnon, J. Fingerprinting intermolecular interactions in molecular crystals. *CrystEngComm* **2002**, *4*, 378–392. [CrossRef]
30. Chandrasekaran, K.; Thilak Kumar, R. Structural, spectral, thermodynamical, NLO, HOMO, LUMO and NBO analysis of fluconazole. *Spectrochim. Acta A Mol. Biomol.* **2015**, *150*, 974–991. [CrossRef] [PubMed]
31. Kazachenko, A.S.; Akman, F.; Vasilieva, N.Y.; Issaoui, N.; Malyar, Y.N.; Kondrasenko, A.A.; Borovkova, V.S.; Miroshnikova, A.V.; Kazachenko, A.S.; Al-Dossary, O.; et al. Catalytic sulfation of betulin with sulfamic acid: Experiment and DFT calculation. *Int. J. Mol. Sci.* **2022**, *23*, 1602. [CrossRef]
32. Kadela-Tomanek, M.; Jastrzębska, M.; Marciniak, K.; Chrobak, E.; Bębenek, E.; Boryczka, S. Lipophilicity, pharmacokinetic properties, and molecular docking study on SARS-CoV-2 target for betulin triazole derivatives with attached 1,4-quinone. *Pharmaceutics* **2021**, *13*, 781. [CrossRef] [PubMed]
33. Choudhary, V.K.; Bhatt, A.K.; Dash, D.; Sharma, N. DFT calculations on molecular structures, HOMO–LUMO study, reactivity descriptors and spectral analyses of newly synthesized diorganotin(IV) 2-chloridophenylacetohydroxamate complexes. *J. Comput. Chem.* **2019**, *40*, 2354–2363. [CrossRef]
34. Govindarajan, M.; Karabacak, M.; Periandy, S.; Tanuja, D. Spectroscopic (FT-IR, FT-Raman, UV and NMR) investigation and NLO, HOMO–LUMO, NBO analysis of organic 2,4,5-trichloroaniline. *Spectrochim. Acta A Mol. Biomol. Spectrosc.* **2012**, *97*, 231–245. [CrossRef] [PubMed]
35. Heredia, C.L.; Ferraresi-Curotto, V.; López, M.B. Characterization of Ptn (n = 2–12) clusters through global reactivity descriptors and vibrational spectroscopy, a theoretical study. *Comput. Mater. Sci.* **2012**, *53*, 18–24. [CrossRef]